Zheng, D.; Madrigal-Madrigal, J.; Chen, H.; Barrera Vilar, D.; Sales Maicas, S. (2017). Multicore fiber-Bragg-grating-based directional curvature sensor interrogated by a broadband source with a sinusoidal spectrum. Optics Letters. 42(18):3710-3713. doi:10.1364/OL.42.003710

Multicore fiber Bragg grating based directional curvature sensor interrogated by broadband source with sinusoidal spectrum

DI ZHENG,[1,2*] JAVIER MADRIGAL,[2] HAILAN CHEN,[2] DAVID BARRERA,[2] AND SALVADOR SALES[2]

[1] *Center for Information Photonics & Communications, School of Information Science & Technology, Southwest Jiaotong University, Chengdu, 610031, China*

[2] *Photonics Research Labs, ITEAM Research Institute, Universitat Politècnica de València, Camino de Vera, s/n, 46022, Valencia, Spain*

**Corresponding author: dzheng@home.swjtu.edu.cn*

Received XX Month XXXX; revised XX Month, XXXX; accepted XX Month XXXX; posted XX Month XXXX (Doc. ID XXXXX); published XX Month XXXX

A simple, spectral-drift-insensitive interrogation scheme for multicore fiber Bragg grating based directional curvature sensor is proposed. The basic principle is to transform the wavelength shift of FBGs into the reflected power variation, which is accomplished by utilizing broadband source with sinusoidal spectrum. The closed-form expression of the relationship between the reflected power of FBG and the corresponding peak wavelength is derived for the first time to our knowledge, therefore the peak wavelength of FBG can be precisely interrogated by using single photodiode. The experimental results show that, with respect to conventional wavelength measurement by optical spectrum analyzer, the demodulated wavelength error by our proposed interrogation scheme is within ±20pm. The proposed scheme is further extended to interrogate the direction and curvature using multicore fiber Bragg grating based curvature sensor, the interrogated curvature with error less than 8% is achieved.

OCIS codes: *(060.3735) Fiber Bragg gratings; (060.2370) Fiber optics sensors.*

http://dx.doi.org/10.1364/OL.99.099999

In recent years, multicore fiber (MCF) featuring more than one cores within a single cladding attracted great interest in the applications such as high-capacity optical transmission networks and microwave photonics systems to cope with the exponential growth of data transmission demand [1-3]. In addition, MCFs have also been given special attention by optical sensing community due to its unique characteristics of compactness, robustness as well as flexibility. MCF based sensors have been widely used in bend/curvature [4,5], shape [6], flow velocity [7], accelerometers sensing [8] and so on.

M. J. Gander et al. report the first demonstration of bend sensing using Bragg gratings written in a two-core optical fiber [9]. The interrogation scheme is based on the monitoring of strain difference between a pair of FBGs by measuring the wavelength shift. Since then, this kind of sensing technique is extended to the two-dimensional curvature and shape sensing using homogeneous or heterogeneous multicore fiber [10,11]. Other interrogation scheme is based on a two-dimensional far-field interferogram, and the bend angle is determined by calculating phase values derived from Fourier analysis of the far-field interferogram [12,13]. Recently, distributed shape sensing using Brillouin scattering in multicore fibers has been reported, too [14,15]. The response to curvature of the Brillouin frequency of outer cores in a MCF provides the capability to retrieve the information of 3D shape.

To date, the overwhelming majority of MCF based sensing rely on the measurement of the wavelength shift of FBG or the fringes moving of interferogram, which resulting in the requirement of expensive measuring equipment, such as optical spectrum analyzer (OSA), and complex data processing algorithms. Although power-based FBG demodulation technique using sinusoidal filtering has been provided, the use of polarization maintaining fiber loop mirror makes system complex and is sensitive to spectral drift of the sinusoidal filtering response [16,17]. In addition, the existing power-based FBG demodulation schemes need two photodetectors to realize the ratio detecting, which increase the system complexity and cost.

In this paper, a novel FBG wavelength interrogation scheme is proposed. A detailed theoretical analysis is conducted firstly, the quantitative relationship between the reflected power of FBG and the corresponding peak wavelength is obtained. Then, the feasibility and performance of the proposed scheme is verified by experimental demonstration. Based on this, the proposed FBG interrogation scheme is extended to the application of curvature sensing using multicore fiber Bragg grating. The results

demonstrated the feasibility of the proposed directional curvature interrogation scheme with the characteristics of cost-effective, high precision and high speed.

The proposed curvature sensing system is shown in Fig.1 (a). The entire system consists of a broadband optical source (BBS) with the sinusoidal spectral profile, a 1×2 optical coupler, two optical circulator, a Fan-in/out device, a MCF and two photodiodes. FBGs were written into three aligned cores of the MCF. Two output ports of the optical coupler are connected to the two outer cores of MCF through Fan-in/out devices.

The basic operation principle is explained as follows: The input BBS signal with the sinusoidal spectral profile is firstly divided into two branches and launched into the MCF; Then, the input signals are reflected by two individual FBGs carrying the information of local curvature; Finally, these reflected signals are routed out by optical circulator and detected by PDs. The intensity of the reflected signal is determined by the center wavelength of the FBG and the relative location with respect to the sinusoidal optical spectrum. When the MCF is bended along the plane of two FBGs, the center wavelength of two FBGs will shift oppositely, and meanwhile the reflected power changes in the form of sinusoidal response. For a given sinusoidal optical spectrum, assumed that the peak intensity and peak position are known, then the central wavelength of FBG can be retrieved from the intensity of reflected signal. By determining the amount of the wavelength shift of FBG, local curvature as well as bending direction can be determined.

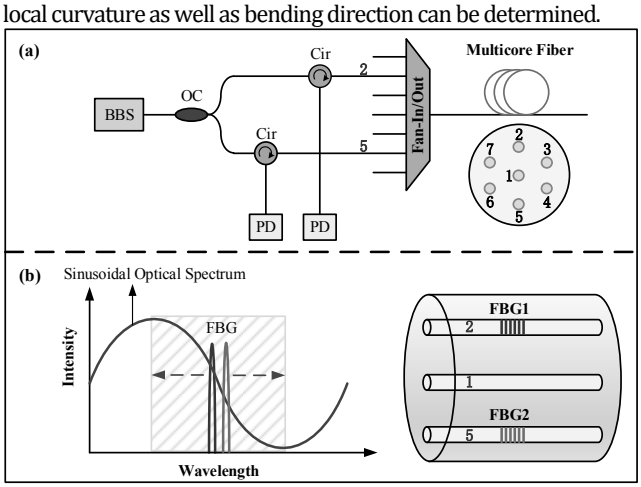

Fig.1. (a) Schematic arrangement of sensor system, (b) Schematic diagram of interrogation. BBS: broadband light source; OC: optical coupler; Cir: optical circulator; PD: photodetector

The detailed theoretical analysis is described as follows. The reflection spectrum of an FBG is approximately expressed by a Gaussian profile:

$$F(\lambda) = R\exp\left[-\frac{(\lambda-\lambda_0)^2}{2\Delta\lambda^2}\right] \quad (1)$$

where R, λ_0 and $\Delta\lambda$ are the peak reflection, center wavelength and the half-width (at 1/e-intensity point) of the FBG Gaussian profile, respectively. It is customary to use the full width at half maximum (FWHM) in place of $\Delta\lambda$, the two are related as

$$\lambda_{FWHM} = 2\sqrt{2\ln 2}\Delta\lambda \quad (2)$$

The spectral profile of broadband optical source is sinusoidal, as can be seen in Fig. 1(b). For a limited wavelength range, the period of the sinusoidal spectrum can be considered constant, so the power spectrum of the optical source is written as:

$$S(\lambda) = S_0\left[V\cos\left(2\pi\frac{\lambda-\lambda_I}{\Delta\lambda_I}\right)+1\right] \quad (3)$$

where S_0, λ_I, $\Delta\lambda_I$ and V are the peak power, center wavelength, period and the visibility of the sinusoidal spectrum, respectively. Therefore, the reflected signal power from the FBG is given by:

$$\begin{aligned} P &= \int_0^\infty S(\lambda)F(\lambda)d\lambda \\ &\approx \left(\frac{\sqrt{2\pi}}{2}\Delta\lambda S_0 R\right)\times\left[V\cos\left(2\pi\frac{\lambda_0-\lambda_I}{\Delta\lambda_I}\right)+1\right] \end{aligned} \quad (4)$$

Here, in order to obtain the closed-form expression of P, the power spectrum density within the reflection band of FBG is considered to be uniform. This is a reasonable approximation when the bandwidth of FBG is far less than the period of the sinusoidal spectrum. Under the above assumption, P varies with the central wavelength of FBG in the form of a sinusoidal response. Provided that the reflection spectrum of the FBG is located around the half-power point of input sinusoidal spectrum and the range of the bending-induced wavelength shift is less than a half of period (i.e. the orange region shown in Fig.1(b)), the central wavelength of the FBG can be accurately calculated by Eq. (4) through measuring the reflected signal power.

The relationship between the wavelength shift of the FBG and the bending-induced axial strain is defined as [9]:

$$\Delta\lambda_B = \lambda_B(1-p_\varepsilon)\varepsilon \quad (5)$$

where ε is the bend-induced strain, λ_B is the initial wavelength when no bending is applied on MCF, p_ε denotes the effective photo-elastic coefficient, which its value is around 0.22 in a standard optical fiber. Therefore, when the bending direction along the plane of two FBGs, the curvature C can be easily obtained through the strain difference between two FBGs [9], which is given as:

$$C = \frac{\varepsilon_{FBG1}-\varepsilon_{FBG2}}{d} \quad (6)$$

where ε_{FBG1} and ε_{FBG1} are the bending-induced strain values of the two cores inscribed FBG1 and FBG2 respectively, d is the distance between the two cores.

In our experiment, a commercial seven-core MCF from Fibercore Ltd. is used for the implementation of the curvature sensing. The MCF has a cladding diameter of 125 μm and the cores are arranged in a hexagonal pattern with one of the cores in the center, as seen in Fig.1(a). The core spacing is 35±0.75 μm and each core has a mode field diameter of 6.4 μm and a numerical aperture of 0.2. In order to increase the photosensitivity, the MCF is hydrogen-loaded at ambient temperature for two weeks at 50 bar pressure. Three cores located at the same plane of the seven-core MCF are selected to inscribe FBGs simultaneously using a 244 nm CW frequency-doubled argon-ion laser, a detailed description of FBG inscription can be found in [3].

The curvature sensor is characterized using the setup shown in Fig.2. This setup is composed by two fiber rotation stages, that rotate the fiber from 0° to 360° with an accuracy of ±5°, one steel strip and two three axis translation stages. The MCF is placed at the top of the steel strip and the FBGs are located in the center of the

steel strip. When the two translation stages approach each other, the metal strip is bended and near uniform curvature are obtained. Two of the six outer cores arranged symmetric to the center core are selected for curvature sensing, the plane of the two cores are parallel to the bending direction.

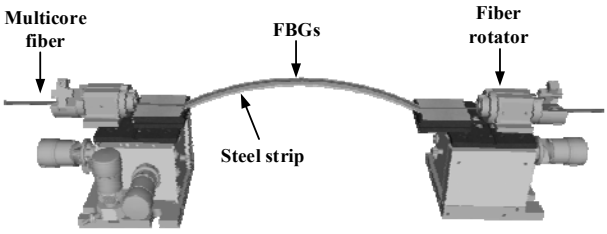

Fig.2. Experimental characterization setup for curvature sensing

In order to obtain a BBS with sinusoidal spectral response, a home-made photonic crystal fiber (PCF) interferometer with the characteristic of temperature insensitive and high stability is employed [18]. The PCF interferometer consists of a short piece of PCF longitudinally spliced between two standard SMFs (SMF-28). A broadband amplified spontaneous emission (ASE) source in combination with a PCF interferometer is utilized to the generation of the desired BBS. The spectral characteristic of BBS is shown in Fig.3 (a). It can be seen that the generated spectrum is fitted quite well to ideal sine function, where the period of the sinusoidal spectrum is 5.1nm. During the experiment, the sinusoidal spectrum can be shifted by bending the PCF interferometer to locate the Bragg wavelength at the right position.

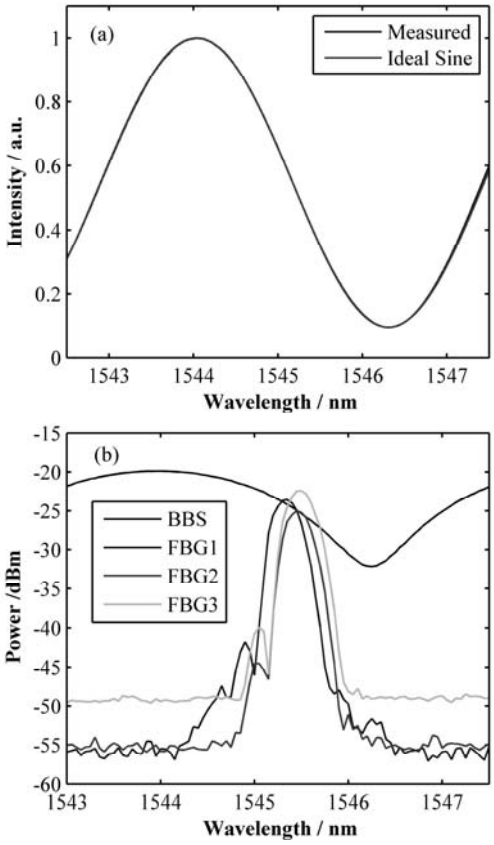

Fig.3. The spectra of (a) BBS and (b) three FBGs

Fig.3 (b) shows the measured reflection spectra of the three FBGs inscribed in three different cores at the same position along the fiber length. The center wavelengths of the three FBGs are all located around the half-power point of the input sinusoidal spectrum. FBG1 and FBG2 written in the two outer cores have almost same FWHMs of 0.2nm and the central wavelength difference of ~0.1 nm. Note that an additional FBG3 is inscribed in central core, its role is to compensate temperature or externally applied axial strain during bending steel strip. It should be pointed out that the proposed curvature interrogation scheme holds for FBG with arbitrary central wavelength as long as the central wavelength of FBGs is not close to the maximum or minimum point of the sinusoidal spectrum, the feasibility of the proposed interrogation method is almost wavelength-independent.

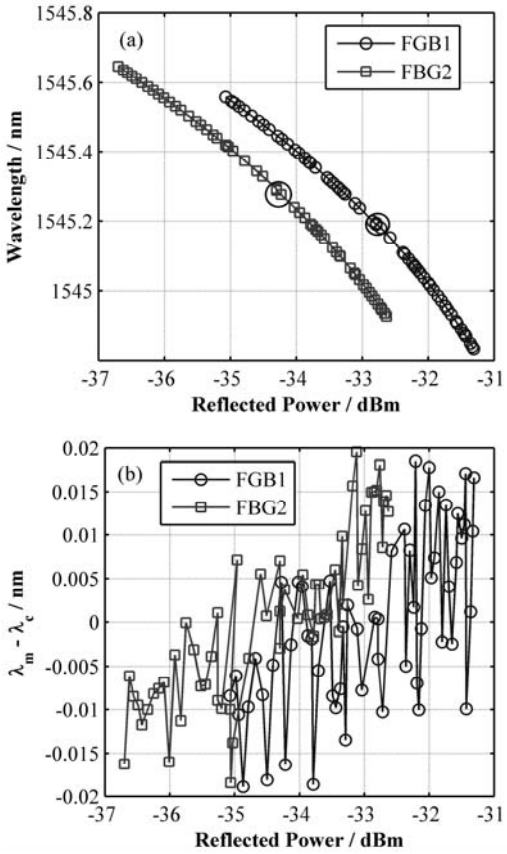

Fig.4. (a) The retrieved center wavelength of two FBGs. (b) The wavelength error between the measurement by OSA λ_m and our proposed interrogating scheme λ_c at different reflected signal power

Fig.4 (a) shows the relationships between the retrieved center wavelength of the two FBGs and the reflected signal power in case that the initial wavelength of two FBGs is located around the half-power point of the input sinusoidal spectrum. The wavelength shift in each FBG shows a good agreement with a sinusoidal behavior. The black circles in Fig.4 (a) denote the initial position of the two FBGs. When the FBG locates at the outer side of the bending fiber, the FBG shifts to longer wavelength with the increasing curvature and the detected signal power decreases. On the contrary, when the FBG locates at the inner side of the bending fiber, a gradually increased signal power means that the FBG shifts to shorter wavelength with increasing curvature.

Fig.4(b) shows the wavelength difference between the retrieved wavelength using Eq. (4) and the measured one by OSA (Ando AQ6317C). It can be seen that the wavelength difference is less than 20pm, which is limited by equipment with the measurement accuracy of ±20pm. Besides, the measure error may come from another two aspects: the spectrum of BBS is not exactly sinusoidal, and a slight fluctuation of the BBS output power.

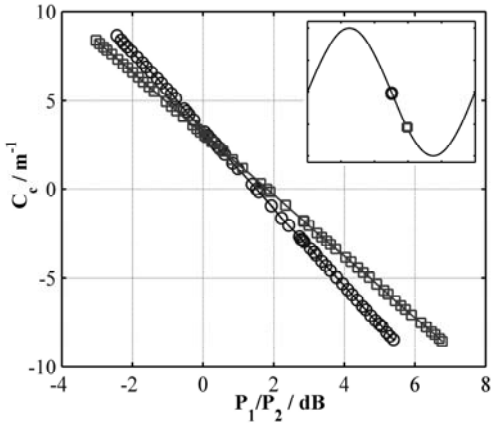

Fig.5. The calculated curvature against power ratio between two FBGs at two different initial locations

Fig. 5 shows the curvature as a function of power ratio between two FBGs. The inset of Fig. 5 shows the two different initial locations of the two FBGs with respect to the input sinusoidal spectrum. The results indicate that there is an excellent linearly relationship between the curvature and power difference between two FBGs, regardless of the initial location of two FBGs. That means even if the input sinusoidal spectrum drifts, the wavelength shifts of two FBGs can still be retrieved, thus the proposed curvature interrogation scheme has strong capability to resist the ambient changes, such as the fluctuation of temperature and polarization. The curvature increases with the power difference, and the bending direction can be distinguished as well from the sign of the curvature. Note that the initial power difference corresponding to the case of no bending is location-dependent, this is due to the central wavelength of two FBGs are not exactly the same, see Fig.3(b).

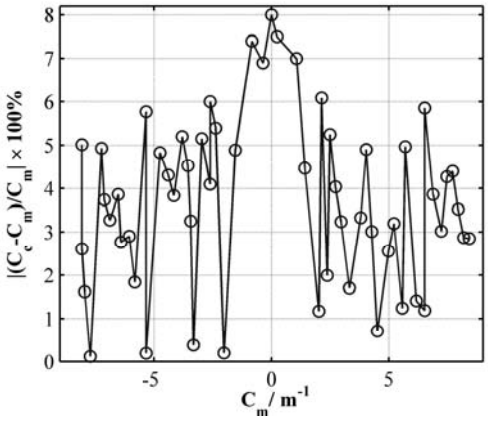

Fig.6. Curvature error at different curvature

The comparison between our proposed curvature interrogation scheme and the conventional curvature interrogation method is carried out, as illustrated in Fig.6. C_c and C_m denote the curvature retrieved by our proposed FBG wavelength interrogation scheme and the conventional measurement method by OSA, respectively. It can be seen that the maximum curvature error is less than 8%, the error can be further reduced by employing more stable BBS with true sinusoidal spectrum. The curvature error at smaller curvature is slightly greater than that at larger curvature, which is ascribed to the fact that the changes of the reflected power is negligible and resulting in the inaccuracy of the measured signal power.

In summary, the analytical relationship between the reflected power of FBG and the corresponding peak wavelength is established taking into account the effects of the profile and bandwidth of FBG. The peak wavelength of FBG can be precisely demodulated by detecting the corresponding reflected power. This novel FBG wavelength interrogation scheme is further expanded to curvature sensing based on multicore fiber Bragg grating. The experimental results demonstrate the feasibility of our proposed scheme with high accuracy and good stability.

Funding. This work was supported in part by the National Natural Science Foundation of China (61405166) and the China Scholarship Council, in part by Generalitat Valenciana (APOSTD/2016/015, GVA PROMETEO 2013/012); Ministerio de Economía y Competitividad (MINECO) (TEC2014-60378-C2-1-R).

References

1. B. Zhu, T.F. Taunay, M. Fishteyn, X. Liu, S. Chandrasekhar, M. F. Yan, J. M. Fini, E. M. Monberg and F. V. Dimarcello, Opt. Express **19**, 16665 (2011).
2. I. Gasulla and J. Capmany, IEEE Photonics J. **4**, 977 (2012).
3. I. Gasulla, D. Barrera, J. Hervás and S. Sales, Sci. Rep. **7**, 41727 (2017).
4. F. M. Araujo, L. A. Ferreira, and J. L. Santos, Appl. Optics **41**, 2401 (2002).
5. D. Barrera, I. Gasulla, and S. Sales, J. Lightwave Technol. **33**, 2445 (2015).
6. J. P. Moore and M. D. Rogge, Opt. Express **20**, 2976 (2012).
7. L. B. Yuan, J. Yang and Z. H. Liu, IEEE Sens. J. **8**, 1114 (2008).
8. A. Fender, W. N. MacPherson, R. R. J. Maier, J. S. Barton, D. S. George, R. I. Howden, G. W. Smith, B. J. S. Jones, S. McCulloch, X. Chen, R. Suo, L. Zhang, and I. Bennion, IEEE Sens. J. **8**, 1292 (2008).
9. M. J. Gander, W. N. MacPherson, R. McBride, J.D.C. Jones, L. Zhang, I. Bennion, P.M. Blanchard, J.G. Burnett, and A. H. Greenaway, Electron. Lett. **36**, 120 (2000).
10. G. M. H. Flockhart, W. N. MacPherson, J. S. Barton, J. D. C. Jones, L. Zhang, and I. Bennion, Opt. Lett. **28**, 387 (2003).
11. H. L. Zhang, Z. F. Wu, P. P. Shum, R. X. Wang, X. Q. Dinh, S. N. Fu, W. J. Tong and M. Tang, J. Optics **18**, 1 (2016).
12. P. M. Blanchard, J. G. Burnett, G. R. G. Erry, A. H. Greenaway, P. Harrison, B. Mangan, J. C. Knight, P. St. J. Russell, M. J. Gander, R. McBride and J. D. C. Jones, Smart Mater. Struc. **9**, 132 (2000).
13. M. J. Gander, D. Macrae, E. A. C. Galliot, R. McBride, J. D. C. Jones, P. M. Blanchard, J. G. Burnett, A. H. Greenaway, M. N. Inci, Opt. Commun. **182**, 115 (2000).
14. Y. Mizuno, N. Hayashi, H. Tanaka, Y. Wada, and K. Nakamura, Sci. Rep. **5**, 11388 (2015).
15. Z. Y. Zhao, M. A. Soto, M. Tang and L. Thevenaz, Opt. Express **24**, 25213 (2016).
16. S. Chung, J. Kim, B. A. Yu and B. Lee, IEEE Photon. Technol. Lett., **13**(12), 1343, (2001).
17. X. Zhang, S. Hu and C. He, MATEC Web of Conferences, **61**, 06010, (2016).
18. D. Barrera, J. Villatoro, V. P. Finazzi, G. A. Cárdenas-Sevilla, V. P. Minkovich, S. Sales and V. Pruneri, J. Lightwave Technol. **28**, 3542 (2010).

REFERENCE

1. B. Zhu, T.F. Taunay, M. Fishteyn, X. Liu, S. Chandrasekhar, M. F. Yan, J. M. Fini, E. M. Monberg, and F. V. Dimarcello, "112-Tb/s Space-division multiplexed DWDM transmission with 14-b/s/Hz aggregate spectral efficiency over a 76.8-km seven-core fiber," Optics Express, 19(17), 16665-16671, 2011.
2. I. Gasulla and J. Capmany, "Microwave Photonics Applications of Multicore Fibers," IEEE Photonics Journal, 4(3), 977-888, 2012.
3. I. Gasulla, D. Barrera, J. Hervás and S. Sales, "Spatial Division Multiplexed Microwave Signal processing by selective grating inscription in homogeneous multicore fibers," Scientific Reports, 7, 41727, 2017.
4. F. M. Araujo, L. A. Ferreira, and J. L. Santos, "Simultaneous determination of curvature, plane of curvature, and temperature by use of a miniaturized sensing head based on fiber Bragg gratings," Applied Optics, 41(13), 2401-2407, 2002.
5. D. Barrera, I. Gasulla, and S. Sales, "Multipoint Two-Dimensional Curvature Optical Fiber Sensor Based on a Nontwisted Homogeneous Four-Core Fiber" IEEE Journal of Lightwave of Technology, 33(12), 2445-2450, 2015.
6. J. P. Moore and M. D. Rogge, "Shape sensing using multi-core fiber optic cable and parametric curve solutions," Optics Express, 20(3), 2976-2973, 2012.
7. L. B. Yuan, J. Yang and Z. H. Liu, "A Compact Fiber-Optic Flow Velocity Sensor Based on a Twin-Core Fiber Michelson Interferometer," IEEE Sensors Journal, 8(7), 1114-1117, 2008.
8. A. Fender, W. N. MacPherson, R. R. J. Maier, J. S. Barton, D. S. George, R. I. Howden, G. W. Smith, B. J. S. Jones, S. McCulloch, X. Chen, R. Suo, L. Zhang, and I. Bennion, "Two-Axis Temperature-Insensitive Accelerometer Based on Multicore Fiber Bragg Gratings," IEEE Sensors Journal, 8(7), 1292-1298, 2008.
9. M. J. Gander, W. N. MacPherson, R. McBride, J.D.C. Jones, L. Zhang, I. Bennion, P.M. Blanchard, J.G. Burnett, and A. H. Greenaway, "Bend measurement using Bragg gratings in multi-core fiber," Electronics Letters 36(2), 120-121, 2000.
10. G. M. H. Flockhart, W. N. MacPherson, J. S. Barton, J. D. C. Jones, L. Zhang, and I. Bennion, "Two-axis bend measurement with Bragg gratings in multicore optical fiber," Optics Letters 28(6), 387–389 (2003).
11. H. L. Zhang, Z. F. Wu, P. P. Shum, R. X. Wang, X. Q. Dinh, S. N. Fu, W. J. Tong and M. Tang, "Fiber Bragg gratings in heterogeneous multicore fiber for directional bending sensing," Journal of Optics, 18, 1-7, 2016.
12. P. M. Blanchard, J. G. Burnett, G. R. G. Erry, A. H. Greenaway, P. Harrison, B. Mangan, J. C. Knight, P. St. J. Russell, M. J. Gander, R. McBride and J. D. C. Jones, "Two-dimensional bend sensing with a single, multi-core optical fibre," Smart Materials and Structures, 9, 132-140, 2000.
13. M. J. Gander, D. Macrae, E. A. C. Galliot, R. McBride, J. D. C. Jones, P. M. Blanchard, J. G. Burnett, A. H. Greenaway, M. N. Inci, "Two-axis bend measurement using multicore optical fibre," Optics Communications, 182, 115-121, 2000.
14. Y. Mizuno, N. Hayashi, H. Tanaka, Y. Wada, and K. Nakamura, "Brillouin scattering in multi-core optical fibers for sensing applications," Scientific Reports, 5, 11388 (2015).
15. Z. Y. Zhao, M. A. Soto, M. Tang and L. Thevenaz, "Distributed shape sensing using Brillouin scattering in multi-core fibers," Optics Express, 24(22), 25213, 2016.
16. S. Chung, J. Kim, B. A. Yu and B. Lee, "A fiber Bragg grating sensor demodulation technique using a polarization maintaining fiber loop mirror," IEEE Photonics Technology Letters, 13(12), 1343-1345, 2001.
17. X. Zhang, S. Hu and C. He, "A fibre Bragg grating interrogation technique based on high birefringence fibre loop mirror and WDM," MATEC Web of Conferences, 61, 06010, (2016).
18. D. Barrera, J. Villatoro, V. P. Finazzi, G. A. Cárdenas-Sevilla, V. P. Minkovich, S.Sales and V. Pruneri, "Low-Loss Photonic Crystal Fiber Interferometers for Sensor Networks," IEEE Journal of Lightwave of Technology, 28(24), 3542-3547, 2010.